UV-cross-linked block copolymers for initiator-free, controlled in situ gelation of electrolytes in dye-sensitized solar cells

ARTICLE *in* JOURNAL OF MATERIALS CHEMISTRY · APRIL 2012

Impact Factor: 7.44 · DOI: 10.1039/C2JM32526H

5 AUTHORS, INCLUDING:

Ngoc Uyen
Ho Chi Minh City University of Science
5 PUBLICATIONS **17** CITATIONS

SEE PROFILE

Journal of Materials Chemistry

Cite this: *J. Mater. Chem.*, 2012, **22**, 18854

www.rsc.org/materials

PAPER

UV-cross-linked block copolymers for initiator-free, controlled *in situ* gelation of electrolytes in dye-sensitized solar cells

Sung Chul Hong,*[a] Ngoc Uyen Nguyen-Thai,[a] Soo Bong Hong[a] and Phil-Hyun Kang[b]

Received 22nd April 2012, Accepted 5th July 2012
DOI: 10.1039/c2jm32526h

In this work, a block copolymer as an initiator- and monomer-free UV-cross-linked component for the controlled *in situ* gelation of electrolytes in dye-sensitized solar cells (DSSCs) is proposed. This block copolymer consists of one block of *p*-hydroxystyrene units and the other block with poly(ethylene oxide-*co*-propylene oxide) side chains. This block copolymer is successfully prepared by means of nitroxide-mediated polymerization, imidization reactions and successive hydrolysis reactions. When a homogeneous mixture of this copolymer and a typical liquid electrolyte (LE) is irradiated with UV, the cross-linking is efficient and controlled. The electrolyte in the DSSCs transforms *in situ* to a gel polymer electrolyte when exposed to UV, affording DSSCs with a relatively high initial solar-to-electricity energy conversion efficiency (η) and improved long-term stability that is significantly greater than that of the DSSCs with LE. These results demonstrate that the electrolyte system containing the UV-cross-linked block copolymer improves the long-term performance of DSSCs and contributes to the development of efficient and stable DSSCs.

Introduction

The solar-to-electricity energy conversion efficiency of dye-sensitized solar cells (DSSCs) with liquid electrolytes recently reached 12%.[1] However, leakage and volatilization of the liquid electrolyte limit the long-term stability and practical success of DSSCs.[2] One approach is to replace the liquid electrolyte with less volatile ionic liquids[3–6] which, unfortunately, do not prevent leakage. Inorganic or organic hole transport materials have been introduced as substitutes for the liquid electrolyte in all-solid-state DSSC configurations.[7–9] However, the limited ionic (generally, I^-/I_3^-) conductivity can result in lower energy conversion efficiency for DSSCs. For the DSSCs to be successful, although contradictory, the electrolyte must have high ionic conductivity and low leakage/volatility.

Gel polymer electrolytes (GPEs), which trap the liquid electrolyte in polymer matrices, can improve ionic conductivity, and provide low vapor pressure and negligible leakage of electrolytes.[2,10–14] In this approach, the efficient penetration of the electrolyte into the nanoporous TiO_2 photoelectrode is a key prerequisite. Kang *et al.* provided an example of wetting behavior by liquid oligomers with multiple hydrogen bonding sites, which allowed efficient pore filling of TiO_2 photoanodes that underwent *in situ* self-solidification during solvent evaporation.[15,16] This phase transformation strategy showed promise as a pathway for high performance and stable DSSCs by improving the interfacial contact between the (pseudo) solid-state electrolyte and the TiO_2 electrode. However, the preparation of the oligomer and the assembly of the DSSC were tedious.

In this work, we propose an *in situ* UV-cross-linked GPE system that differs from a simple GPE, which is a mixture of a liquid electrolyte and a gelling agent, such as a simple electrolyte-philic polymer. We designed our electrolyte system to be a liquid that can easily penetrate into TiO_2 nanopores and then undergo an *in situ* transformation to a pseudo-solid state when exposed to appropriate UV irradiation. In this work, we specifically designed the architecture and functionality of a UV-sensitive oligomeric cross-linker for *in situ* GPE systems. This oligomeric UV-cross-linker is targeted to eliminate undesirable initiators and low molecular weight residues after the curing process, which otherwise could reduce the long-term stability of the DSSCs.[17] This oligomeric cross-linker also maximizes the mechanical/thermal stability of the GPE through the efficient formation of a covalent 3-D cross-linked network (Scheme 1). Unlike conventional heat-generating polymerization or thermal-cross-linking processes, this UV-cross-linking system provides a low-temperature curing process which avoids thermal damage to the dyes or other critical components of the DSSCs. In addition, UV irradiation may be beneficial to improve the efficiency of DSSCs through the production of a high density of TiO_2 surface states,[18] although UV may also have a negative effect on dye in the presence of air or water at elevated temperature.[19]

[a]*Department of Nano Science and Technology, Sejong University, Seoul 143-747, Republic of Korea. E-mail: sunghong@sejong.ac.kr; Fax: +82-2-3408-4342; Tel: +82-2-3408-3750*
[b]*Radiation Research Division for Industry and Environment, Korea Atomic Energy Institute, Jeongeup-si, Jeollabuk-do 580-185, Republic of Korea*

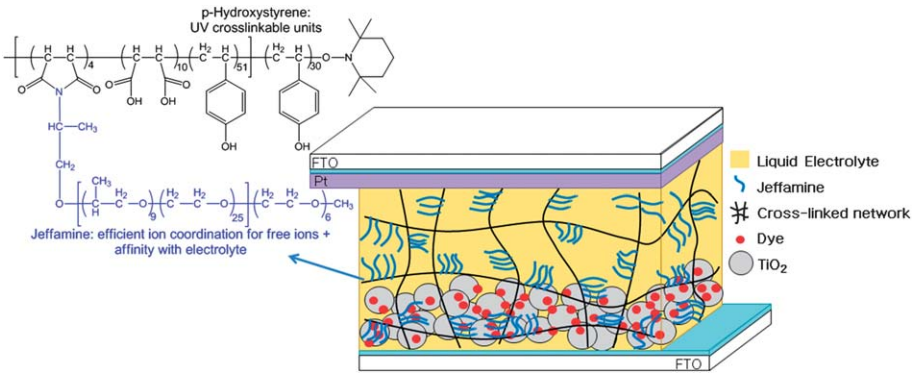

Scheme 1 Schematic illustration of the DSSC assembled *via* an *in situ* cross-linking of the gel-polymer electrolyte employing the oligomeric UV-cross-linker proposed in this study.

Experimental procedures

Materials

p-Acetoxystyrene (*p*AS, 96%, Aldrich) was purified by passing through a column filled with neutral alumina and stored under nitrogen in a freezer. Maleic anhydride (MA, 99%, Aldrich), 2,2′-azobisisobutyronitrile (AIBN, 98%, Samchun Chemicals), 2,2,6,6-tetramethyl-1-peperidine 1-oxyl (TEMPO, 98%, Aldrich) and anisole (99%, Aldrich) were used as received. Poly(ethylene oxide-*co*-propylene oxide) with mono amine end-groups (Jeffamine, M-2070, methoxy-poly(ethylene oxide-*co*-propylene oxide)-2-propylamine, molecular weight approximately 2000 g mol^{-1}) was purchased from Hustman Chemical Company. The propylene oxide/ethylene oxide (PO/EO) molar ratio was 10/31. Tetrahydrofuran (THF, 99.5%, Samchun Chemicals), methanol (99.5%, Samchun Chemicals), ethanol (95.0%, Samchun Chemicals), toluene (99.5%, Samchun Chemicals), *N*,*N*-dimethylformamide (DMF, 99.5%, Samchun Chemicals), hexane (95.0%, Samchun Chemicals), dimethyl sulfoxide (DMSO, 99.8%, Samchun Chemicals), acetic anhydride (Ac_2O, 99%, Aldrich), triethylamine (TEA, 99%, Aldrich) and pyridine (99%, Aldrich) were used without further purification. TiO_2 (ENB Corp., 20 nm particle size) and Ru-dye (N719, Solaronix) were used to fabricate the DSSCs. Additionally, 1-propyl-3-methyl imidazolium iodide (PMII, >99%, C-Tri), guanidinium thiocyanate (GuSCN, >97%, Aldrich), iodine (I_2, >99.8%, Aldrich), 4-*tert*-butylpyridine (TBP, 99%, Aldrich), acetonitrile (ACN, 99.5%, Duksan) and valeronitrile (Val, 99.5%, Aldrich) were used without further purification as components for the liquid electrolytes. All additional chemicals were purchased from Aldrich and used without purification.

Preparation of poly(maleic anhydride-*co*-*p*-acetoxystyrene)-*block*-poly(*p*-acetoxystyrene) (PASMA)

MA (1.18 g, 1.20×10^{-2} mol), *p*AS (15 mL, 9.80×10^{-2} mol), AIBN (0.07 g, 4.26×10^{-4} mol), TEMPO (0.165 g, 1.056×10^{-3} mol) and anisole (1.5 mL) were added to a 100 mL Schlenk flask and degassed through three freeze–pump–thaw cycles ([*p*AS] : [MA] : [AIBN] : [TEMPO] = 300 : 28 : 1 : 2.4). The reactor was immersed in an oil bath at 135 °C. A syringe was used to collect samples from the flask at specific intervals. The samples were diluted with THF and analyzed by methods such as gas chromatography (GC) and gel permeation chromatography (GPC). After polymerization for 2 hours, the reactor was removed from the oil bath and cooled to room temperature. The product, a viscous solution, was diluted with THF, and the polymer was precipitated from methanol and dried under vacuum at 60 °C for 12 hours (PASMA, $M_n = 14\,500$ g mol^{-1}, $M_w/M_n = 1.23$).

Preparation of poly(maleimide-*co*-*p*-acetoxystyrene)-*block*-poly(*p*-acetoxystyrene) functionalized with Jeffamine (PASMI-*g*-Jeffamine)

A total of 50 mL of a 10 wt% solution of PASMA (5.0 g, 4.52×10^{-3} mol of MA) in anhydrous DMF was placed in a 150 mL three-necked flask equipped with a Dean–Stark trap and stirred magnetically under nitrogen. The concentration of the PASMA in the DMF was controlled at 10 wt% to avoid an inter-chain cyclization reaction during the imidization reaction.[20] The Jeffamine (9.03 g, 4.52×10^{-3} mol) was dissolved in anhydrous DMF in a flask and degassed through three freeze–pump–thaw cycles. Then, a syringe was used to add the Jeffamine solution to the PASMA solution. The mixture was stirred at 60 °C for 3 hours, and acetic anhydride (0.9 mL, 9.5×10^{-3} mol) and triethylamine (0.7 mL, 5.0×10^{-3} mol) were added. The reactor was immersed in an oil bath at 100 °C for 7 hours. The PASMI-*g*-Jeffamine was precipitated with cold methanol and washed with cold methanol. The product, a powder, was dried under vacuum at 60 °C (PASMI-*g*-Jeffamine, $M_n = 22\,500$ g mol^{-1}, $M_w/M_n = 1.25$).

Preparation of poly(maleic acid-*co*-*p*-hydroxystyrene)-*block*-poly(*p*-hydroxystyrene) functionalized with Jeffamine (PHSMI-*g*-Jeffamine)

PASMI-*g*-Jeffamine (7 g), 1,4-dioxane (44 mL), water (3.5 mL), and sulfuric acid (7 drops) were placed in a 100 mL round bottom flask. The reactor was immersed in an oil bath that was preset to the specific reaction temperature (90 °C). After 24 hours, the mixture was removed from the oil bath and cooled to room temperature. The product, a white powder, was precipitated from deionized water and dried under vacuum at 80 °C for 24 hours.

Preparation and characterization of electrolytes

Osram Dulux Blue UVA lamps (9 W – 78 × 4, 350–430 nm) were used in a UV-box (15 cm × 15 cm) to irradiate the electrolytes. The separation between the electrolytes and the UV lamps was 5 cm in every experiment for uniform irradiation. A standard liquid electrolyte was prepared by adding 0.7 M PMII, 0.03 M I_2 (0.05 M), 0.05 M GuSCN and 0.5 M TBP to a mixture of ACN/Val (7/3 v/v), and stirring at room temperature for 12 hours. The polymer electrolytes were prepared by dissolving the oligomeric UV-cross-linkers (PHSMI-*g*-Jeffamine) in the liquid electrolyte as described in Table 1.

Fabrication of DSSCs

A standard procedure for the fabrication of DSSCs was as follows (cell active area = 0.4 cm^2, Scheme 2): fluorine-doped tin oxide (FTO) conducting glass (TEC8, Pilkington, 8 Ω $\square^{-1}$, glass thickness of 2.3 mm) was pre-cleaned with ethanol. The FTO glass substrate was spin-coated with 0.15 M titanium (IV) bis-(ethylacetoacetato) diisopropoxide solution in 1-butanol and sintered at 500 °C for 10 minutes. The transparent conducting glass was coated with TiO_2 pastes by the doctor-blade technique and sintered at 500 °C for 30 minutes. For the adsorption of dye, the annealed TiO_2 electrodes were immersed in absolute ethanol containing 0.5 mM of N-719 dye (Solaronix) at 60 °C for 3 hours. Pt counter electrodes were prepared separately by drop casting 7 mM H_2PtCl_6 $6H_2O$ in 2-propanol solution and sintering at 400 °C for 20 minutes. The dye-adsorbed TiO_2 electrode and the Pt counter electrode were assembled with 25 μm-thick Surlyn (Solaronix 1170-25). An electrolyte solution was introduced into the cell through a drilled hole (1 mm in diameter) on the counter electrode. The holes were sealed with Surlyn and a cover glass. The DSSCs with the separators were fabricated by inserting the membranes before assembling the TiO_2 electrode and the Pt counter electrode. The DSSCs were exposed to UV irradiation for different lengths of time to form DSSCs with GPE.

Characterizations

The monomer conversion was determined with a gas chromatograph (Shimadzu GC 2010AF) equipped with an FID detector and a ValcoBond VB-wax 30 m column. The molecular weights and molecular weight distributions of the polymers were determined by a Shimadzu LC-20A GPC with PSS columns (styrogel HR 2, 4, 5) and a Shimadzu RID-10A refractive index detector. Proton nuclear magnetic resonance (^{1}H-NMR) measurements were performed with a Bruker 500 MHz instrument; $CDCl_3$ and DMSO-d_6 were the solvents. Fourier transform infrared spectroscopy (FT-IR) was performed with a Nicolet 380 spectrometer. The viscosity of the gel electrolytes was measured with a programmable cone and plate viscometer (spindle CPE-52, DV-III+Pro, Brookfield Engineering) that was equipped with a thermostable water bath. Solar-to-electricity energy conversion efficiency (η%) was measured without masking by using a 2 × 2 Class A ASTM E 927-05 solar simulator (Newport Co., 150 W Xenon lamp) under 1 SUN (AM 1.5) illumination. The photoelectrochemical characteristics of the DSSCs were investigated with electrochemical impedance spectroscopy (EIS, Solartron Frequency Response Analyzer 1260) coupled with a potentiostat/galvanostat (Solartron Electrochemical Interface 1287) at room temperature. The EIS spectra were measured over a frequency range from 0.01 to 10^6 Hz. The impedance parameters (charge-transfer resistances) were analyzed by using Z-view software to fit the impedance spectra. Ionic conductivities (σ) were calculated with the following equation (eqn (1)),

$$\text{Ionic conductivity } (\sigma) = L/AR \quad (1)$$

where L is the distance between the electrodes (25 μm) and A is the active area (0.4 cm^2). The resistance (R) was evaluated from the intercept of the Nyquist plot with the real axis of the impedance spectrum. Electron lifetimes (τ_n) were calculated with the following equation (eqn (2)),[21]

$$\tau_n = 1/2\pi f_{min} \quad (2)$$

where f_{min} is the minimum frequency of the mid-frequency peak.

Results and discussion

We designed the oligomeric cross-linker to have UV-sensitive *p*-hydroxystyrene units in one block and Jeffamine side chains in the other block. Jeffamine was introduced because it has high ion coordination capability and generated high concentrations of effective free ion conducting species.[22] In addition, Jeffamine endowed the copolymer with good miscibility with the polar components in the liquid electrolyte. The *p*-hydroxystyrene units were used as UV-sensitive functional groups. These *p*-hydroxystyrene units are very sensitive to UV irradiation and instantly

Table 1 Compositions of electrolytes tested in this study

Designation	PHSMI-*g*-Jeffamine[a] (g)	Jeffamine/PHSMA[b] (g)	PHSMA[b] (g)	Jeffamine/PSMA[c] (g)	PSMA[c] (g)	LE[d] (g)
G	0.5	—	—	—	—	2
M	—	0.14/0.36	—	—	—	2
H	—	—	0.5	—	—	2
SM[e]	—	—	—	0.14/0.36	—	2
SH[e]	—	—	—	—	0.5	2

[a] PHSMI-*g*-Jeffamine = Jeffamine grafted poly(maleic acid-*co*-*p*-hydroxystyrene)-*block*-poly(*p*-hydroxystyrene). [b] PHSMA = poly(maleic acid-*co*-*p*-hydroxystyrene)-*block*-poly(*p*-hydroxystyrene). [c] PSMA = poly(maleic anhydride-*co*-styrene)-*block*-polystyrene. [d] Liquid electrolyte (LE): PMII (0.7 M), I_2 (0.05 M), GuSCN (0.05 M) and TBP (0.5 M) in acetonitrile/valeronitrile (7/3 v/v). [e] Polymers did not dissolve in liquid electrolyte solution; heterogeneous mixture.

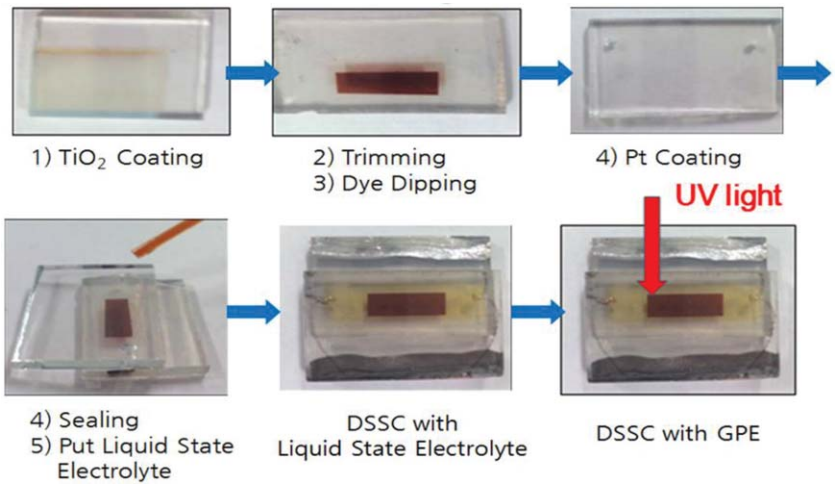

Scheme 2 Schematic representation of the fabrication procedure for the DSSCs employing the UV-cross-linked gel polymer electrolyte (GPE).

generate radicals for efficient cross-linking between chains even in a diluted solution (Scheme 3).[23]

Polyethers, such as poly(ethylene oxide) (PEO) and poly(propylene oxide) (PPO), have been used as polymer electrolytes for electrochemical devices such as batteries, display devices and sensors in the presence of high concentrations of free conducting ions.[24–26] However, the high degree of crystallinity (approximately 80%) and the low melting point (approximately 65 °C) of PEO often result in limited ionic conductivity and thermal stability, which interfere with practical applications of PEO-based electrolytes.[13,24,27] The need to design a PEO-based copolymer with minimum crystallinity and maximum thermal stability motivated the incorporation of PEO or PPO segments into copolymers. High ionic conductivity (approaching 10^{-3} S cm^{-1} at 25 °C) has been achieved by incorporating PEO-based copolymers into electrolytes.[13,28,29] Kim *et al.* also reported that UV-cross-linkable PEO precursors with azide groups afforded GPE with improved ionic conductivity and mechanical properties,[30] although the precursors contained only two terminal cross-linkable units. These previous studies provided a reasonable background for this study, where the UV-cross-linker was designed with Jeffamine side chains in the block copolymer.

This author has reported a facile and scalable synthetic method to prepare functional oligomers by a controlled/"living" polymerization technique (CRP).[31–35] This method yielded oligomers with block chain architecture, where the role and functionality of each segment was easily and precisely designed. The target UV-cross-linker was synthesized through this CRP process.

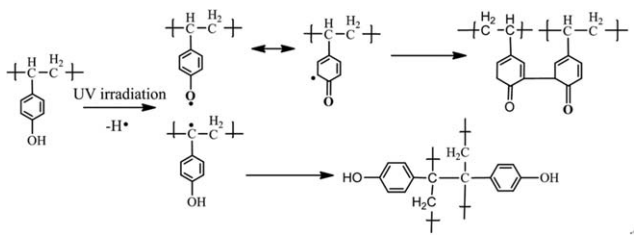

Scheme 3 Representative cross-linking mechanism of the *p*-hydroxystyrene units under UV irradiation.[23]

The three steps in the synthesis of the UV-cross-linkable copolymer (PHSMI-*g*-Jeffamine) are described in Scheme 4. First, a convenient one-pot nitroxide-mediated radical polymerization (NMP) process was used to produce PASMA (Scheme 4, first step). MA tends to form charge transfer complexes with the styrenic comonomer, which leads to more alternating copolymerization behavior. During the NMP process, this copolymerization tendency resulted in the preferential consumption of MA at the beginning of the polymerization and the formation of the MA functionalized polystyrenic blocks.

MA was incorporated completely into the polymers during the polymerization time of 30 minutes, while the conversion of *p*AS was only 34% (Fig. 1a). In principle, this first block contained approximately 14 units of MA (assuming that the initiation efficiency of AIBN was 1). The mole ratio of MA to *p*AS in this first copolymer block was approximately 1 to 3.6, which indicated that there were 51 units of *p*AS in the first block. After MA was consumed completely, the remaining *p*AS continued to polymerize and produce the second block (Fig. 1a). This procedure represented a very convenient one-step preparation of the functionalized block copolymers. The conversion of *p*AS between 1 and 2 hours during polymerization was 50% (Fig. 1a), which indicated that the second block contained approximately 30 units of *p*AS.

Fig. 1b represents the evolution of the number-average molecular weight (M_n) and the polydispersity indices (M_w/M_n) during *p*AS conversion. A relatively good agreement between the theoretical and experimental molecular weights with conversion and narrow molecular weight distributions (PDI = 1.25) ensured a successful CRP process and confirmed the formation of PASMA.

In the FT-IR spectra of the PASMA copolymers (Fig. 2b), the band near 1760 cm^{-1} demonstrated the stretching vibrations of the carbonyl group from MA and *p*AS. The broad band near 1210 cm^{-1} originated from the C–O–C stretching vibration of the maleic anhydride units.[36,37] The stretching vibration peaks of the aromatic C–H, methylene C–H and C=C rings (3050 cm^{-1}, 2930–2850 cm^{-1}, and 1500 cm^{-1}, respectively) represented the presence of *p*AS. The ^{1}H-NMR spectroscopy spectrum (Fig. 3a) showed all of the characteristic signals from the PASMA, which confirmed the successful preparation of the PASMA.

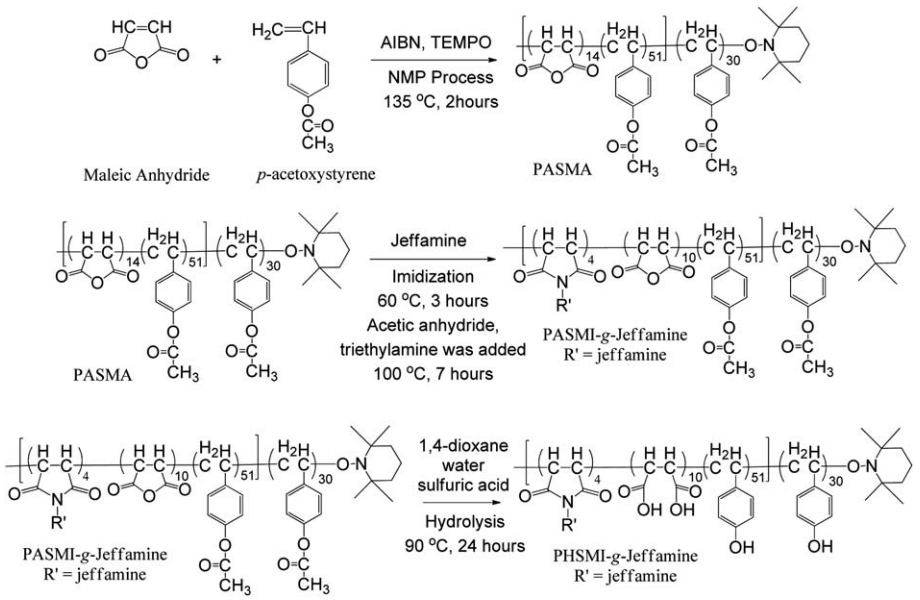

Scheme 4 Schematic representation of the preparation of Jeffamine grafted UV-cross-linked block oligomer (PHSMI-*g*-Jeffamine): the preparation of the poly(maleic anhydride-*co*-*p*-acetoxystyrene)-*block*-poly(*p*-acetoxystyrene) (first step, PASMA); the grafting of the Jeffamine onto the PASMA (second step, PASMI-*g*-Jeffamine); and the hydrolysis of the graft copolymer to produce the PHSMI-*g*-Jeffamine (third step).

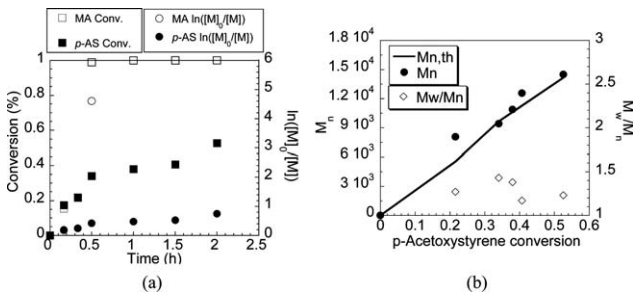

Fig. 1 Kinetic plots (a) and evolution of M_n and M_w/M_n *versus* conversion of *p*-acetoxystyrene (*p*AS, (b)) for the copolymerization of *p*AS and maleic anhydride (MA). *Polymerization condition*: [*p*AS] : [MA] : [AIBN] : [TEMPO] = 300 : 28 : 1 : 2.4; temperature = 135 °C; time = 2 hours.

Jeffamine was incorporated into the block copolymer by utilizing the reactivity of MA through the imidization reaction, which produced block copolymers that were decorated with Jeffamine brushes in one block (PASMI-*g*-Jeffamine) (Scheme 4, second step). The successful incorporation of the Jeffamine was confirmed by the characteristic cyclic imide vibration at 1700 cm^{-1} (Fig. 2c),[20] although a small peak at approximately 1670 cm^{-1} (carbonyl vibration of free carboxyl acid) indicated partial ring opening.[20,38] The presence of Jeffamine in PASMI-*g*-Jeffamine was also confirmed by the broad C–O and C–H vibration peaks of Jeffamine at approximately 1000–1200 cm^{-1} and 2500–3100 cm^{-1} (Fig. 2a and c, arrows). The ^{1}H-NMR spectra also revealed the successful formation of PASMI-*g*-Jeffamine by the presence of the terminal methoxy protons (3.3 ppm) and methylene protons of ethylene oxide repeating units (3.5 ppm) of Jeffamine.

The imidization of the maleic anhydride units with the primary amine of Jeffamine followed two consecutive reactions: a reversible ring opening of maleic anhydride groups to produce maleamic acid groups and an irreversible intra-chain ring closing to form the corresponding maleimide groups with the separation of water.[39,40] In this study, one of the important challenges was to find an optimum condition that provides the maximum number of grafted Jeffamine in PASMI-*g*-Jeffamine.

First, we investigated the effect of the reaction temperature and time without any additional catalyst. As shown in Fig. 4, the number of grafted Jeffamine in PASMI-*g*-Jeffamine increased with time and temperature. However, no specific increase in the number of grafted Jeffamine units was observed after 200 minutes and at temperatures above 100 °C, where the product was PASMI-*g*-Jeffamine with approximately 1.8 Jeffamine chains.

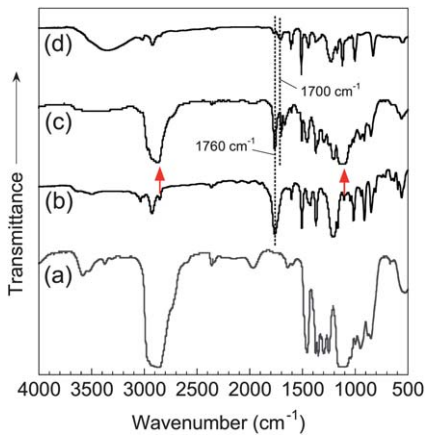

Fig. 2 Fourier transform infrared (FT-IR) spectra of poly(ethylene oxide-*co*-propylene oxide)-*block*-poly(propylene oxide) (Jeffamine, (a)), poly(maleic anhydride-*co*-*p*-acetoxystyrene)-*block*-poly(*p*-acetoxystyrene) (PASMA, (b)), Jeffamine graft on PASMI (PASMI-*g*-Jeffamine, (c)) and hydrolyzed PHSMI-*g*-Jeffamine (d): arrows in (c) indicate peaks originated from Jeffamine.

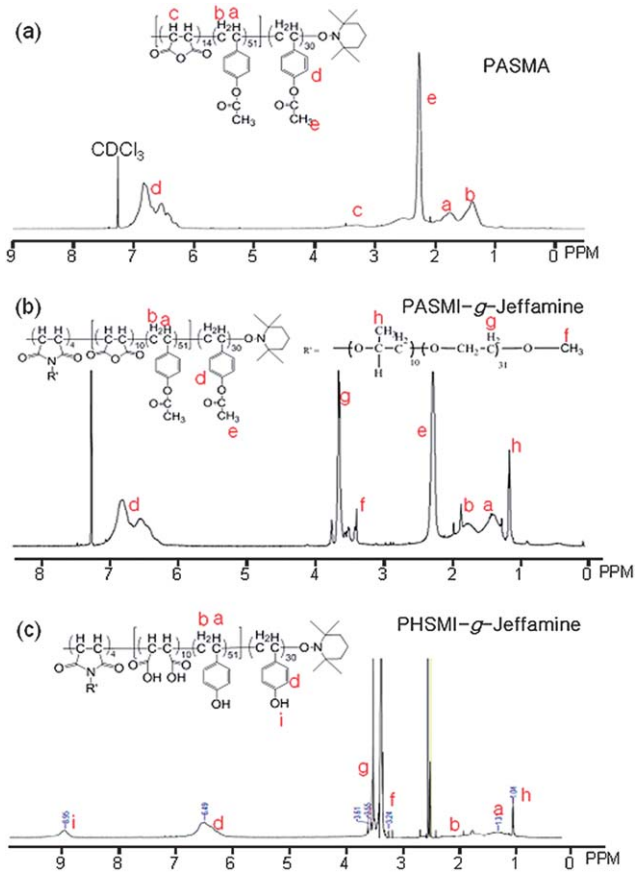

Fig. 3 Proton nuclear magnetic resonance (^{1}H-NMR) spectra of poly(maleic anhydride-*co*-*p*-acetoxystyrene)-*block*-poly(*p*-acetoxystyrene) (PASMA, (a)), Jeffamine grafted poly(maleimide-*co*-*p*-acetoxystyrene)-*block*-poly(*p*-acetoxystyrene) (PASMI-*g*-Jeffamine, (b)) and Jeffamine grafted poly(maleic acid-*co*-*p*-hydroxystyrene)-*block*-poly(*p*-hydroxystyrene) (PHSMI-*g*-Jeffamine, (c)).

The release of water during the intra-chain ring-closing step was indispensable to the formation of the cyclic imide. Therefore, the use of a dehydrating agent improved the reaction efficiency. However, the simple introduction of a dehydrating agent (Ac_2O) reduced the number of grafted Jeffamine units (0.8 Jeffamine per chain, Table 2, experiment number 2) relative to the imidization reaction without a catalyst (1.8 Jeffamine per chain, Table 2, experiment number 1). This result was consistent with the observations of Yang and Hsiao,[41] which were explained by the decomposition of poly(amic acid) in the presence of pure acetic anhydride. Therefore, the introduction of tertiary amines such as pyridine[41] and triethylamine (TEA)[20] was attempted.

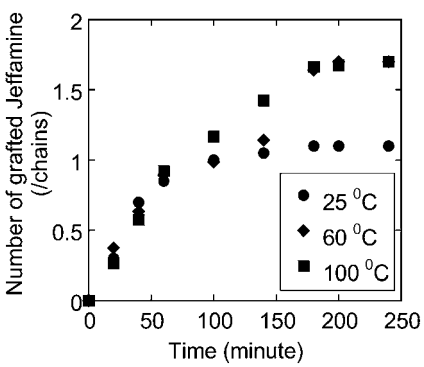

Fig. 4 Evolution of the number of grafted Jeffamine chains with different imidization times determined by proton nuclear magnetic resonance (^{1}H-NMR) analysis. *Reaction condition*: [MA in PASMA] : [Jeffamine] = 1 : 1.

The number of grafted Jeffamine units increased from 0.8 (experiment 2 in Table 2) to 2.7 with Ac_2O/pyridine (experiment 3 in Table 2) and 3.3 with Ac_2O/TEA (experiment 4 in Table 2), which indicated that the imidization reaction was more efficient. According to the mechanism proposed by previous authors,[20,39,42] TEA is a stronger nucleophile than pyridine, and TEA is more efficient in its ability to abstract acidic protons from succinamic acid and acetic acid during ring-closure reactions. However, it should also be noted that the number of grafted Jeffamine chains was limited to approximately 4 (4.0 chains according to GPC analysis and 3.3 chains by ^{1}H-NMR analysis), probably because the neighboring *p*AS units provide steric hindrance.[42]

The block copolymer with *p*-hydroxystyrene units was prepared by the hydrolysis reaction of PASMI-*g*-Jeffamine in 1,4-dioxane in the presence of a strong acid catalyst (Scheme 4, third step). The successful hydrolysis reaction was confirmed by FT-IR (Fig. 2d) and ^{1}H-NMR (Fig. 3c) analyses. In the FT-IR spectra, the presence of the strong O–H stretching vibration at approximately 3100–3600 cm^{-1} from the carboxylic acid groups of maleic acid and the hydroxyl group of *p*-hydroxystyrene was evidence of the successful hydrolysis reaction (Fig. 2d). The disappearance of the carbonyl stretching vibration around 1760 cm^{-1} (which was assigned to the carbonyl group of *p*AS) was further evidence of the hydrolysis reaction. The apparent imide stretching vibration at approximately 1700 cm^{-1} supported the high resistance of the imide group to acidic hydrolysis. The ^{1}H-NMR spectrum also revealed a new hydroxy proton peak at 9.0 ppm (Fig. 3c). The conversion of *p*AS to *p*-hydroxystyrene, which was calculated from the integration ratio between the aromatic proton (6.5 ppm) and hydroxy proton (9.0 ppm), was above 90%, indicating that PASMI-*g*-Jeffamine almost completely transformed to PHSMI-*g*-Jeffamine.

To investigate the effects of Jeffamine and *p*-hydroxystyrene units in the UV-cross-linker, five GPEs that contained different types of cross-linkers, *i.e.*, PHSMI-*g*-Jeffamine, a Jeffamine–PHSMA mixture, PHSMA, poly(maleic anhydride-*co*-styrene)-*block*-polystyrene (PSMA), and a Jeffamine–PSMA mixture, were tested along with the LE (Table 1). The chemical structures and abbreviations of the cross-linkers listed in Table 1 are illustrated in Scheme 5.

The degree of cross-linking and the viscosity behaviors of the GPEs with different UV dosages are presented in Fig. 5. To determine the degree of cross-linking, pre-weighed electrolyte solutions containing 20 wt% of the oligomeric UV-cross-linker were cast onto a glass surface. The samples were exposed to UV irradiation for different lengths of time, washed with THF and dried under vacuum. The degree of cross-linking was calculated from the mass ratio between the remaining and original polymers.

The mixture of PSMA and Jeffamine–PSMA was not soluble in the LE components (SM and SH in Table 1) and did not undergo gelation regardless of the UV dosage. Although several authors have reported that polystyrene can be UV-cross-

Table 2 Number of Jeffamine units grafted on poly(maleic anhydride-*co*-*p*-acetoxystyrene)-*block*-poly(*p*-acetoxystyrene) under different reaction conditions[a]

	Catalyst			GPC analysis		^{1}H-NMR analysis		
Exp no.	Ac_2O	Pyridine	TEA	M_n[b] ($\times 10^{-3}$ g mol^{-1})	Number of Jeffamine[c] (per chain)	I_f	I_d	Number of Jeffamine[d] (per chain)
1	—	—	—	17.0	1.3	0.031	1.87	1.8
2	2.0	—	—	15.5	0.5	0.016	2.34	0.8
3	2.0	1.1	—	18.5	2.0	0.040	1.64	2.7
4	2.0	—	1.1	22.5	4.0	0.091	1.87	3.3

[a] *Reaction conditions*: solvent, anhydrous DMF; time 10 hours; temperature, 100 °C; Ac_2O = acetic anhydride; TEA = triethylamine. [b] M_n, number average molecular weight of PASMI-*g*-Jeffamine; M_n of PASMA was 14 500 g mol^{-1}. [c] The number of Jeffamine chains grafted on a copolymer was calculated from GPC: Number of Jeffamine (per chain) $= \frac{(M_n - M_n \text{ of PASMA})}{M_{\text{Jeffamine}}} = \frac{(M_n - 14\,500)}{2000}$. [d] The number of Jeffamine chains grafted on a copolymer was calculated from ^{1}H-NMR: Number of Jeffamine (per chain) $= \frac{I_f/3}{I_d/4} \times 81$, where I_f and I_d are integration of methoxy proton and benzyl proton (please refer to Fig. 3).

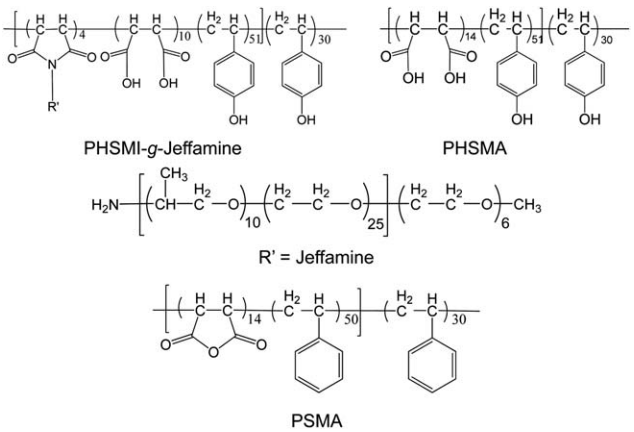

Scheme 5 Chemical structures and abbreviations of the cross-linkers employed in Table 1.

linked,[43,44] the cross-linking efficiency of polystyrene appears to be very low in diluted and/or heterogeneous systems. These behaviors suggest the importance of the *p*-hydroxystyrene-based cross-linker for the efficient formation of GPE.

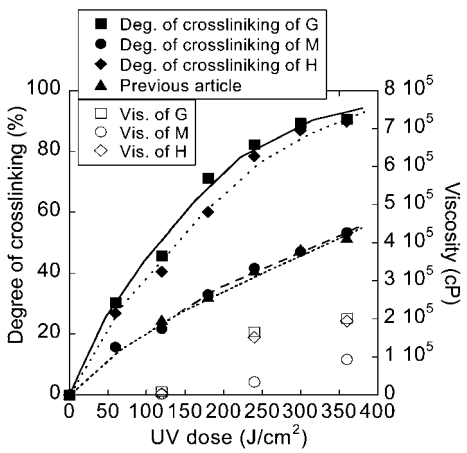

Fig. 5 Degree of cross-linking and viscosity behaviors of gel polymer electrolyte with different UV dosages for PHSMI-*g*-Jeffamine (G), Jeffamine–PHSMA (M), PHSMA (H), and those of polyethylene glycol–trimethylolpropane triacrylate.[45]

Efficient cross-linking under UV radiation was observed for the polymers with *p*-hydroxystyrene units (G, M, and H in Table 1) that contained LE, even in diluted systems (Fig. 5). The mixtures of PHSMI-*g*-Jeffamine (G in Table 1) with LE exhibited over 90% cross-linking after a UV dose of 360 J cm^{-2}, which represents very efficient UV-cross-linking (Table 3). The viscosity values of G were up to 200 000 cP, which indicated a gel state. These results for the cross-linking capability were much higher than the results that were reported previously for photo-cross-linked polymeric electrolyte systems such as poly(ethylene glycol)/trimethylolpropane triacrylate (TMPTA),[45] where the degree of cross-linking was only 52%. In this work, the degree of cross-linking for Jeffamine–PHSMA (M-UV in Table 3) that contained LE was limited to approximately 43% because the free Jeffamine was extracted out with THF during the washing step of the experiment. These results provide clear support for the beneficial architecture of PHSMI-*g*-Jeffamine, where covalent grafts of Jeffamine effectively solubilize the PHSMI and improve the homogeneity and cross-linking efficiency. In comparison, the PHSMA (H-UV in Table 3) exhibited a high degree of cross-linking (approximately 90%) naturally due to its high content of *p*-hydroxystyrene units.

It should also be emphasized that the degree of cross-linking increased continuously with the UV dose (Fig. 5). The results indicated that the degree of cross-linking (and the viscosity) of the GPEs was controlled by adjusting the UV dosage. This behavior is beneficial for the optimization of the initial performance of the DSSC and its long-term stability.

To understand the electronic and ionic transport processes in DSSCs, EIS was employed to investigate the electrochemical properties (Fig. 6).[2,45] Ohmic series resistance (R_s), resistance of the charge-transfer process at Pt electrode/electrolyte interfaces (R_1), resistance of the charge-transfer process at TiO_2 electrode/dye/electrolyte interfaces (R_2) and Warburg diffusion impedance (R_3) showing the Nernst diffusion of I_3^- in the electrolyte were determined by fitting the spectra with an equivalent circuit (Fig. 6a); the values are summarized in Table 3.

The presence of cross-linkers in LE apparently changed the properties and the performance of DSSCs (G, M, and H DSSCs in Table 3). Prior to UV irradiation, the ionic conductivity values of the electrolytes with cross-linkers (2.27 mS cm^{-1} for G,

Table 3 Characteristics of electrolytes in dye-sensitized solar cells employing different cross-linkers

Designation[a]	Degree of crosslinking (%)	Viscosity (cP)	R_s (Ω)	R_1 (Ω)	R_2 (Ω)	R_3[b] (Ω)	Ionic conductivity (mS cm^{-1})	τ_n[c] (ms)
LE	0	830	2.22	1.16	3.08	0.67	9.57	7.98
G	0	1050	2.80	1.83	2.84	2.82	2.27	10.04
M	0	720	2.98	2.99	2.02	6.27	1.08	12.64
H	0	1000	2.69	2.44	2.20	5.52	1.16	10.04
LE-UV[d]	0	830	1.80	0.97	2.47	0.78	8.22	5.03
G-UV[d]	89.8	200 000	2.50	2.56	2.41	5.57	1.15	15.92
M-UV[d]	43.4	93 000	2.54	2.17	2.13	6.46	1.05	12.64
H-UV[d]	90.0	194 000	2.86	2.08	1.93	9.96	0.66	15.92

[a] Please refer Table 1 for the designation of electrolytes. [b] Ionic diffusion resistance. [c] Lifetime of photoinduced electrons. [d] UV dosage (360 J cm^{-2}) was applied to the DSSCs.

1.08 mS cm^{-1} for M, and 1.16 mS cm^{-1} for H in Table 3) were lower than the values for LE (9.57 mS cm^{-1} for LE in Table 3) due to the presence of the insulating polymers. Obviously, insulating cross-linkers in LE afforded an electrolyte with high viscosity that limited the diffusion of ionic species, leading to increased R_3 and R_1 values. However, G DSSC exhibited the lowest R_3 values among DSSCs with the cross-linkers, suggesting improved ionic conductivity by grafting Jeffamine chains on the cross-linker backbone. Interestingly, the existence of cross-linkers brought relatively lower R_2 values than that of LE DSSC, where the cross-linkers probably improved the electric contact between electrolytes and TiO_2 electrode/dye as previous research demonstrated.[46] Prolonged electron lifetimes (τ_ns) were also observed in the presence of cross-linkers (τ_n values of G, M, and H DSSCs *versus* that of LE DSSC in Table 3), due to reduced collision frequency between electrons in TiO_2 and I_3^-. It is worth noting that τ_n for M DSSC was the highest among the DSSCs, probably due to relatively easy penetration and coating of the TiO_2 structure with free low molecular weight Jeffamine.

The lower ionic conductivities resulted in slightly lower η values for the DSSCs with G, M, and H electrolytes (6.1% for G, 6.2% for M, and 5.6% for H in Table 4 and Fig. 7) compared with the efficiency of the DSSC with the reference LE (7.4% for LE in Table 4). G DSSC exhibited a relatively high η value (6.1%), suggesting that the TiO_2 photoanode was wetted efficiently by the LE with the PHSMI-*g*-Jeffamine as a cross-linker.

UV irradiation slightly decreased ionic conductivity of LE (9.57 mS cm^{-1} for LE DSSC *versus* 8.22 mS cm^{-1} for LE-UV DSSC in Table 3). On nanocrystalline TiO_2, the absorbed UV photon led to the electron excitation from the valance band to the conduction band, leaving behind positive holes. The accumulation of positive charge on the TiO_2 particles caused a positive shift in the conduction band,[47,48] which, in turn, increased the electron injection rate from dyes. This effect played a role in reduced charge-transfer resistances (3.08 Ω for LE DSSC *versus* 2.47 Ω for LE-UV DSSC, Table 3), increased J_{sc} (14.6 mA cm^{-2} for LE DSSC *versus* 15.6 mA cm^{-2} for LE-UV DSSC, Table 4), and decreased V_{oc} (0.748 V for LE DSSC *versus* 0.687 V for LE-UV DSSC, Table 4). The excited electron in TiO_2 possibly reacted with oxidized species (I_3^-) to afford I^-,[49] leading to a decrease in the concentration of I_3^-. Consequently, R_3 increased (0.67 Ω for LE DSSC *versus* 0.78 Ω for LE-UV DSSC, Table 3), as previously reported.[50] However, at the same time, N719 dye may also degrade under UV irradiation,[19] which overall resulted in inferior η values (7.4% for LE DSSC *versus* 6.9% for LE-UV DSSC, Table 4).

In the presence of cross-linkers, through the dosage of UV, the ionic conductivity of the DSSCs further decreased due to the formation of the cross-linked network structure. The formation of the network increased the viscosity of the GPE and limited the charge transport capability (higher R_3 values for the UV DSSCs

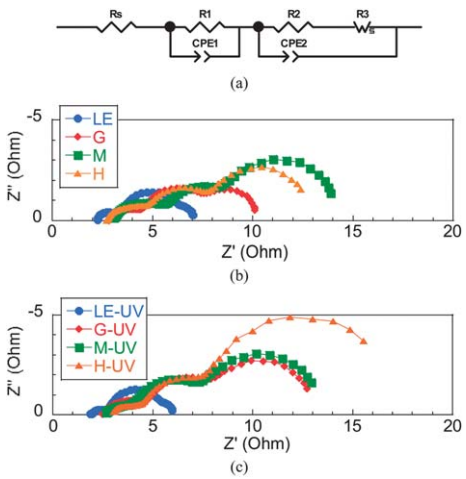

Fig. 6 Equivalent circuit model of DSSCs (a) and Nyquist plots of impedance spectra at the open-circuit photo-potential of the dye-sensitized solar cells with the liquid electrolyte (LE), PHSMI-*g*-Jeffamine (G), Jeffamine–PHSMA (M), and PHSMA (H) electrolytes before UV irradiation (b) and after UV irradiation of 360 J cm^{-2} (c): please refer to Table 1 for the designation of the electrolytes.

Table 4 Characteristics of dye-sensitized solar cells employing different cross-linkers

Designation[a]	V_{oc} (V)	J_{sc} (mA cm^{-2})	FF (%)	η (%)
LE	0.748	14.6	67.3	7.4
G	0.707	17.0	50.5	6.1
M	0.717	16.6	52.4	6.2
H	0.667	16.4	50.7	5.6
LE-UV[b]	0.687	15.6	64.8	6.9
G-UV[b]	0.687	16.4	44.2	5.0
M-UV[b]	0.657	14.7	50.0	4.8
H-UV[b]	0.667	16.6	34.1	3.8

[a] Please refer to Table 1 for the designation of electrolytes. [b] UV dosage (360 J cm^{-2}) was applied to the DSSCs.

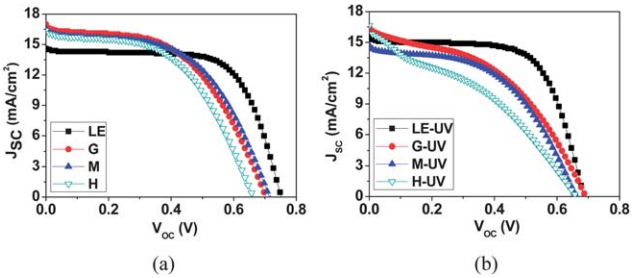

Fig. 7 Photocurrent density–voltage curves of the dye-sensitized solar cells with the liquid electrolyte (LE), PHSMI-*g*-Jeffamine (G), Jeffamine–PHSMA (M), and PHSMA (H) electrolytes before UV irradiation (a) and after UV irradiation of 360 J cm^{-2} (b): please refer to Table 1 for the designation of the electrolytes.

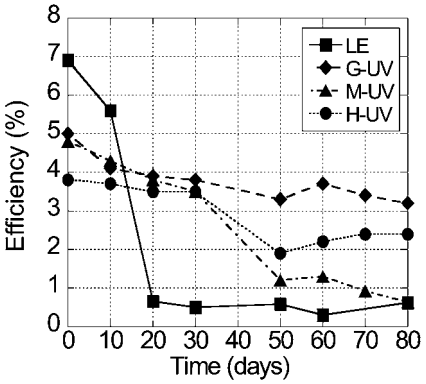

Fig. 8 Long-term behavior of the solar-to-electricity energy conversion efficiency of the DSSCs employing the liquid electrolyte (LE), PHSMI-*g*-Jeffamine (G-UV), Jeffamine–PHSMA (M-UV), and PHSMA (H-UV) electrolytes after UV irradiation of 360 J cm^{-2}: please refer to Table 1 for the designation of the electrolytes.

than those of DSSCs without UV irradiation, Table 3 and Fig. 6),[51] which also resulted in prolonged τ_n values of G-UV, M-UV, and H-UV DSSCs (Table 3).[52] In addition to the plausible degradation of dye under UV irradiation, the lower charge transport capability resulted in inferior η values of UV DSSCs to those of DSSCs before UV irradiation (Table 4).

Although the viscosity of the GPE in the G-UV DSSC (200 000 cP in Table 3) was the highest among the GPEs, the ionic conductivity of the G-UV DSSC (1.15 mS cm^{-1}) was unexpectedly high, which demonstrated the advantages of the PHSMI-*g*-Jeffamine cross-linker. The η value of the G-UV DSSC decreased approximately 18% through the UV irradiation (5.0% for G-UV DSSC *versus* 6.1% for G DSSC, Table 4 and Fig. 7). However, the amount of the reduction in the η value for G-UV DSSC was the lowest among the UV irradiated DSSCs (22% and 32% reduction for η values of M-UV DSSC and H-UV DSSC, respectively). The result well demonstrated excellent initial performances of G-UV DSSC after UV irradiation.

The improvements in the long-term stability of the DSSCs with the GPEs were obvious in comparison with the DSSC with the standard LE (Fig. 8). As shown in Fig. 8, the η value of the DSSC with LE decreased dramatically with time and reached almost 0% after 20 days of storage. This behavior demonstrated serious evaporation or leakage of LE at the current DSSC fabrication conditions. The long-term stability of the M-UV DSSC was also insufficient; the value of η decreased continuously during storage (approximately 85% decrease in cell efficiency after 80 days). The Jeffamine phase simply dispersed in the PHSMA-based electrolyte not only interrupted the UV gel formation procedure and ion-conducting pathways but also was insufficient to prevent leakage and volatilization of LE. The PHSMA homopolymer provided more efficient gel formation (H-UV in Table 3, viscosity of 194 000 cP) and much improved DSSC stability with time (approximately 36% loss of cell efficiency after 80 days, Fig. 8). However, H-UV DSSC exhibited a very low η value (2.4% after 80 days). Most importantly, the η value of the G-UV DSSC was the highest among the DSSCs after 80 days, also exhibiting improved long-term stability. The crossover point of the η values for the LE DSSC and G-UV DSSC was observed at 12 storage days. The Jeffamine side chains, along with *p*-hydroxystyrene units in the main chain, together formed an efficient and homogeneous gel of G-UV DSSC, which in turn improved not only the short-term but also the long-term performances of the DSSC.

Conclusions

Block copolymers with UV-sensitive *p*-hydroxystyrene units in one block and poly(ethylene oxide-*co*-propylene oxide) side chains in the other block were prepared successfully through a combination of nitroxide mediated polymerization, imidization reactions and successive hydrolysis reactions. Homogeneous mixtures of the block copolymers with typical liquid electrolyte (LE) components exhibited efficient and controlled cross-linking under UV irradiation, even in dilute systems. The LE with the block copolymers exhibited over 90% cross-linking after UV irradiation of 360 J cm^{-2}. The viscosity was as high as 200 000 cP, which indicated a gel state. The electrolyte mixture was introduced into a dye-sensitized solar cell (DSSC) and underwent *in situ* gelation after UV. The product was a DSSC with a gel polymer electrolyte (GPE) that exhibited a relatively high initial solar-to-electricity energy conversion efficiency (η value of 5.0%). More importantly, the η values of the DSSC after 80 days demonstrated a significant improvement in the long-term stability compared with that of the DSSC with LE. The crossover point of the η values for the LE DSSC and the G-UV DSSC was observed at 12 days. These results demonstrated that the DSSCs with the *in situ* UV-cross-linkable GPE provide the DSSCs with an improved combination of short- and long-term performance, which may contribute to the commercial success of DSSCs.

Acknowledgements

This research was supported by the Basic Science Research Program through the National Research Foundation of Korea (NRF) funded by the Ministry of Education, Science and Technology (2012005345). This research was also supported by the Nuclear R&D program of the Korean Science and Engineering Foundation and the Ministry of Education, Science and Technology.

References

1 A. Hagfeldt, G. Boschloo, L. Sun, L. Kloo and H. Pettersson, *Chem. Rev.*, 2010, **110**, 6595.
2 Y. Wang, *Sol. Energy Mater. Sol. Cells*, 2009, **93**, 1167.

3 Y. Bai, Y. Cao, J. Zhang, M. Wang, R. Li, P. Wang, S. M. Zakeeruddin and M. Graetzel, *Nat. Mater.*, 2008, **7**, 626.
4 R. Kawano, H. Matsui, C. Matsuyama, A. Sato, M. A. B. H. Susan, N. Tanabe and M. Watanabe, *J. Photochem. Photobiol., A*, 2004, **164**, 87.
5 J. Reiter, J. Vondrák, J. Michálek and Z. Mička, *Electrochim. Acta*, 2006, **52**, 1398.
6 P. Wang, S. M. Zakeeruddin, J. E. Moser and M. Grätzel, *J. Phys. Chem. B*, 2003, **107**, 13280.
7 Q. Li, J. Zhao, B. Sun, B. Lin, L. Qiu, Y. Zhang, X. Chen, J. Lu and F. Yan, *Adv. Mater.*, 2012, **24**, 945.
8 H. Wang, X. Zhang, F. Gong, G. Zhou and Z. S. Wang, *Adv. Mater.*, 2012, **24**, 121.
9 Y. Saito, N. Fukuri, R. Senadeera, T. Kitamura, Y. Wada and S. Yanagida, *Electrochem. Commun.*, 2004, **6**, 71.
10 S.-W. Rhee and W. Kwon, *Korean J. Chem. Eng.*, 2011, **28**, 1481.
11 W. Wu, J. Li, F. Guo, L. Zhang, Y. Long and J. Hua, *Renewable Energy*, 2010, **35**, 1724.
12 B. Li, L. Wang, B. Kang, P. Wang and Y. Qiu, *Sol. Energy Mater. Sol. Cells*, 2006, **90**, 549.
13 A. F. Nogueira, C. Longo and M. A. De Paoli, *Coord. Chem. Rev.*, 2004, **248**, 1455.
14 O. A. Ileperuma, M. A. K. L. Dissanayake and S. Somasundaram, *Electrochim. Acta*, 2002, **47**, 2801.
15 M.-S. Kang, J. H. Kim, J. Won and Y. S. Kang, *J. Phys. Chem. C*, 2007, **111**, 5222.
16 Y. J. Kim, J. H. Kim, M.-S. Kang, M. J. Lee, J. Won, J. C. Lee and Y. S. Kang, *Adv. Mater.*, 2004, **16**, 1753.
17 M. K. Parvez, I. In, J. M. Park, S. H. Lee and S. R. Kim, *Sol. Energy Mater. Sol. Cells*, 2011, **95**, 318.
18 B. A. Gregg, S.-G. Chen and S. Ferrere, *J. Phys. Chem. B*, 2003, **107**, 3019.
19 H. G. Agrell, J. Lindgren and A. Hagfeldt, *Sol. Energy*, 2003, **75**, 169.
20 S.-S. Lee and T. O. Ahn, *J. Appl. Polym. Sci.*, 1999, **71**, 1187.
21 R. Kern, R. Sastrawan, J. Ferber, R. Stangl and J. Luther, *Electrochim. Acta*, 2002, **47**, 4213.
22 J. Yoon, D. K. Kang, J. Won, J.-Y. Park and Y. S. Kang, *J. Power Sources*, 2012, **201**, 395.
23 S. Uppalapati, S. Chada, M. H. Engelhard and M. Yan, *Macromol. Chem. Phys.*, 2010, **211**, 461.
24 J. Kang, W. Li, X. Wang, Y. Lin, X. Xiao and S. Fang, *Electrochim. Acta*, 2003, **48**, 2487.
25 G. P. Kalaignan, M.-S. Kang and Y. S. Kang, *Solid State Ionics*, 2006, **177**, 1091.
26 J. B. Xia, F. Y. Li, C. H. Huang, J. Zhai and L. Jiang, *Sol. Energy Mater. Sol. Cells*, 2006, **90**, 944.
27 M. J. Reddy and P. P. Chu, *Electrochim. Acta*, 2002, **47**, 1189.
28 M. S. Kang, J. H. Kim, Y. J. Kim, J. Won, N. G. Park and Y. S. Kang, *Chem. Commun.*, 2005, 889.
29 M. S. Kang, Y. J. Kim, J. Won and Y. S. Kang, *Chem. Commun.*, 2005, 2686.
30 J. Hwan Koh, J. Kwan Koh, N.-G. Park and J. H. Kim, *Sol. Energy Mater. Sol. Cells*, 2010, **94**, 436.
31 S. C. Hong, J. E. Shin, H. J. Choi, H. H. Gong, K. Kim and N.-G. Park, *Ind. Eng. Chem. Res.*, 2010, **49**, 11393.
32 H. J. Choi, J. E. Shin, G.-W. Lee, N.-G. Park, K. Kim and S. C. Hong, *Curr. Appl. Phys.*, 2010, **10**, S165.
33 Y. J. Lee, Y. Jang, K. Cho, S. Pyo, D.-H. Hwang and S. C. Hong, *J. Nanosci. Nanotechnol.*, 2009, **9**, 7161.
34 J. H. Woo, M. Park, S.-S. Lee and S. C. Hong, *J. Nanosci. Nanotechnol.*, 2009, **9**, 1872.
35 I. H. Choi, M. Park, S.-S. Lee and S. C. Hong, *Eur. Polym. J.*, 2008, **44**, 3087.
36 A. Boztuğ and S. Basan, *J. Appl. Polym. Sci.*, 2003, **89**, 296.
37 G. Chen, Y. Zhang, X. Zhou and J. Xu, *Appl. Surf. Sci.*, 2006, **253**, 1107.
38 H. Fang, F. Mighri and A. Ajji, *J. Appl. Polym. Sci.*, 2008, **109**, 3938.
39 H.-Y. Liu, K. Cao, Y. Huang, Z. Yao, B.-G. Li and G.-H. Hu, *J. Appl. Polym. Sci.*, 2006, **100**, 2744.
40 G. Schmidt-Naake, H. G. Becker and M. Klak, *Macromol. Symp.*, 2001, **163**, 213.
41 C.-P. Yang and S.-H. Hsiao, *J. Appl. Polym. Sci.*, 1985, **30**, 2883.
42 M. Rätzsch, *Prog. Polym. Sci.*, 1988, **13**, 277.
43 Y. J. Jang, Y. H. Jang, M. Steinhart and D. H. Kim, *Chem. Commun.*, 2012, **48**, 507.
44 Y. Wang, J. Liu, S. Christiansen, D. H. Kim, U. Gosele and M. Steinhart, *Nano Lett.*, 2008, **8**, 3993.
45 S. R. Kim, M. K. Parvez, I. In, H. Y. Lee and J. M. Park, *Electrochim. Acta*, 2009, **54**, 6306.
46 D. Qin, Y. Zhang, S. Huang, Y. Luo, D. Li and Q. Meng, *Electrochim. Acta*, 2011, **56**, 8680.
47 S. Ferrere and B. A. Gregg, *J. Phys. Chem. B*, 2001, **105**, 7602.
48 A. Hagfeldt, U. Björkstén and M. Grätzel, *J. Phys. Chem.*, 1996, **100**, 8045.
49 M. Carnie, D. Bryant, T. Watson and D. Worsley, *Int. J. Photoenergy*, 2012, **2012**, 1.
50 J. H. Park, K. J. Choi, S. W. Kang, Y. Seo, Y. S. Kang, J. Kim and S.-S. Lee, *J. Photochem. Photobiol., A*, 2010, **213**, 1.
51 F. M. Wang, C. H. Chu, C. H. Lee, J. Y. Wu, K. M. Lee, Y. L. Tung, C. H. Liou, Y. Y. Wang and C. C. Wan, *Int. J. Electrochem. Sci.*, 2011, **6**, 1100.
52 Y. Yang, H. Hu, C.-H. Zhou, S. Xu, B. Sebo and X.-Z. Zhao, *J. Power Sources*, 2011, **196**, 2410.